THE JOURNAL OF BIOLOGICAL CHEMISTRY
Vol. 280, No. 29, Issue of July 22, pp. 27111–27120, 2005
Printed in U.S.A.
© 2005 by The American Society for Biochemistry and Molecular Biology, Inc.

Peroxisomal Import of Human Alanine:glyoxylate Aminotransferase Requires Ancillary Targeting Information Remote from Its C Terminus*[S]

Received for publication, March 11, 2005, and in revised form, May 19, 2005
Published, JBC Papers in Press, May 23, 2005, DOI 10.1074/jbc.M502719200

Pia A. J. Huber, Graeme M. Birdsey, Michael J. Lumb, David T. R. Prowse, Tommy J. Perkins, Daniel R. Knight, and Christopher J. Danpure‡

From the Department of Biology, University College London, Gower Street, London WC1E 6BT, United Kingdom

Although human alanine:glyoxylate aminotransferase (AGT) is imported into peroxisomes by a Pex5p-dependent pathway, the properties of its C-terminal tripeptide (KKL) are unlike those of any other type 1 peroxisomal targeting sequence (PTS1). We have previously suggested that AGT might possess ancillary targeting information that enables its unusual PTS1 to work. In this study, we have attempted to locate this information and to determine whether or not it is a characteristic of all vertebrate AGTs. Using the two-hybrid system, we show that human AGT interacts with human Pex5p in mammalian cells, but not yeast cells. Using (immuno)fluorescence microscopic analysis of the distribution of various constructs expressed in COS cells, we show the following. 1) The putative ancillary peroxisomal targeting information (PTS1A) in human AGT is located entirely within the smaller C-terminal structural domain of 110 amino acids, with the sequence between Val-324 and Ile-345 being the most likely candidate region. 2) The PTS1A is present in all mammalian AGTs studied (human, rat, guinea pig, rabbit, and cat), but not amphibian AGT (*Xenopus*). 3) The PTS1A is necessary for peroxisomal import of human, rabbit, and cat AGTs, but not rat and guinea pig AGTs. We speculate that the internal PTS1A of human AGT works in concert with the C-terminal PTS1 by interacting with Pex5p indirectly with the aid of a yet-to-be-identified mammal-specific adaptor molecule. This interaction might reshape the tetratricopeptide repeat domain allosterically, enabling it to accept KKL as a functional PTS1.

Alanine:glyoxylate aminotransferase (AGT,[1] EC 2.6.1.44) catalyzes the transamination of the intermediary metabolite glyoxylate to glycine. A deficiency of AGT, as occurs in the hereditary disease primary hyperoxaluria type 1, allows glyoxylate to be oxidized to oxalate instead. The resulting increased synthesis and excretion of oxalate leads to the deposition of insoluble calcium oxalate in the kidney and urinary tract and, ultimately, renal failure (1). AGT is normally peroxisomal in human liver, but in a subset of primary hyperoxaluria type 1 patients it is mistargeted to mitochondria (2). Although the molecular basis of the peroxisome-to-mitochondrion mistargeting of AGT in primary hyperoxaluria type 1 has been subjected to extensive investigation (3–6), its normal targeting to peroxisomes has received much less attention (7, 8).

Peroxisomal import of human AGT is dependent on the presence of the type 1 peroxisomal targeting sequence (PTS1) receptor Pex5p, but not the PTS2 receptor Pex7p (7). However, several features of the peroxisomal targeting of AGT are unusual when compared with the targeting of other peroxisomal proteins. The C-terminal tripeptide of human AGT is KKL (9), which has a two-out-of-three match with the prototypical consensus PTS1 of (S/A/C)(K/R/H)(L/M) (10, 11). KKL is necessary for peroxisomal targeting of human AGT but insufficient to direct the peroxisomal targeting of reporter proteins, such as bacterial chloramphenicol acetyltransferase or firefly luciferase (7, 12). This has led to the suggestion that additional targeting information may be necessary beyond that provided by the C-terminal tripeptide (7).

PTS1s are recognized by, and interact with, the tetratricopeptide repeat (TPR) domain located in the C-terminal part of Pex5p (13, 14). Crystallographic analysis of human Pex5p bound to a synthetic hexapeptide ending in SKL showed that a small uncharged residue is required in the −3 position (15). Lysine, which is the residue at −3 in human AGT, does not fit this description, being large and positively charged. Therefore, it is not surprising that human AGT does not appear to interact directly with human Pex5p in the yeast two-hybrid assay (8). However, what is surprising is that the peroxisomal import of human AGT is still Pex5p-dependent (7). Although numerous tripeptides have been shown to be able to act as PTS1s, albeit in a highly context-dependent fashion, KKL has never been shown to either act as a PTS1 or interact directly with Pex5p (for example, see Refs. 16–19). In addition, to our knowledge, KKL has not yet been found at the C terminus of any other peroxisomal protein.

Further evidence that the human AGT PTS1 behaves very differently from other PTS1 sequences is shown by the observation that normal human AGT (ending in KKL) does not compete with other PTS1 proteins for peroxisomal import in a transient overexpression system, whereas mutated human AGT (ending in SKL) and GFP-SKL do (8). In addition, the peroxisomal import of

* This work was supported by grants from the Wellcome Trust and the Leverhulme Trust. The costs of publication of this article were defrayed in part by the payment of page charges. This article must therefore be hereby marked "*advertisement*" in accordance with 18 U.S.C. Section 1734 solely to indicate this fact.

[S] The on-line version of this article (available at http://www.jbc.org) contains Supplemental Table SI.

‡ To whom correspondence should be addressed. Tel./Fax: 44-20-7679-7936; E-mail: c.danpure@ucl.ac.uk.

[1] The abbreviations used are: AGT, alanine:glyoxylate aminotransferase (EC 2.6.1.44); *Cp*, guinea pig (*Cavia porcellus*); *Fc*, cat (*Felix cattus*); GFP, green fluorescent protein or enhanced green fluorescent protein; *Hs*, human (*Homo sapiens*); MTS, mitochondrial targeting sequence; *Oc*, rabbit (*Oryctolagus cuniculus*); PBS, phosphate-buffered saline; PTS1, type 1 peroxisomal targeting sequence; PTS1A, ancillary peroxisomal targeting information that enables the C-terminal tripeptide of human AGT (*i.e.* KKL) to function as a PTS1; PTS2, type 2 peroxisomal targeting sequence; *Rn*, rat (*Rattus norvegicus*); TPR, tetratricopeptide repeat; *Xl*, *Xenopus* (*Xenopus laevis*).

Downloaded from http://www.jbc.org/ at Murdoch University (CAUL) on May 5, 2019

AGT-KKL, but not AGT-SKL or GFP-SKL, is markedly inhibited by overexpression of human Pex5p (8).

Unlike the C termini of most other PTS1 proteins, the C termini of mammalian AGTs are poorly conserved. For example, it is KKL in human (9) and marmoset (20), HRL in guinea pig (21), SQL in rabbit (20), NKL in rat (22), mouse (23), and cat (24), HKL in dog (EMBL accession number AAEX01037931/2, *Canis familiaris* chromosome 25 contig 37930/1), and SKL in cow (EMBL accession number AV605720, *Bos taurus* cDNA). This evolutionary variability differs from archetypal PTS1 proteins, such as urate oxidase, the C terminus of which (*i.e.* SRL) is conserved in rat, rabbit, mouse, pig, and baboon, or acyl-CoA oxidase, the C terminus of which (*i.e.* SKL) is conserved in rat, mouse, guinea pig, human, and koala.

A complicating factor with AGT, but as far as we are aware no other peroxisomal protein, is that its intracellular compartmentalization varies between different mammalian species (25–30). For example, in the human, rabbit, and guinea pig hepatocytes, AGT is peroxisomal. However, in the cat and dog, AGT is mainly mitochondrial with only a small proportion peroxisomal. In other mammals, such as marmoset and rat, AGT is more evenly distributed between both peroxisomes and mitochondria. Some non-mammalian vertebrates do not target AGT to peroxisomes at all. For example, in *Xenopus laevis*, AGT is mitochondrial and cytosolic. Interestingly, the C terminus of *Xenopus* AGT (*i.e.* KKM), although very similar to the KKL of human AGT, appears to be unable to act as a PTS1 (28).

Since the original discovery of the PTS1, it has become increasingly clear that a wide variety of tripeptides can target proteins to peroxisomes, albeit in a context-dependent manner. Context can be provided by the type of cell (particularly the species from which it is derived) or the nature of the cargo (*i.e.* the protein to be imported). In the case of the former, Pex5p from different species might have different PTS1 requirements (16, 31). Whereas in the case of the latter, amino acids in close proximity (*i.e.* within 10–20 residues) to the C-terminal tripeptide can markedly influence the properties of, and allowable residues within, the PTS1 (16, 17, 32–35). The importance of specific residues near the C terminus appears to be particularly important if the C-terminal tripeptide deviates from the conservative consensus PTS1 (16). However, even the canonical PTS1 SKL can be inhibited by the close proximity of acidic amino acids (12). Human AGT is unusual in that the degeneracy of its PTS1 occurs in the same protein and cellular context. Human AGT can be targeted to peroxisomes not only by KKL, but also by all the other tripeptides found in mammalian AGTs (*i.e.* NKL, SQL, HRL, and SKL) as well as the glycosomal targeting sequence SSL (7). However, there are limits to the degeneracy of the allowable PTS1s in human AGT; SEL, DEL, LLL, and the *Xenopus* C terminus, KKM, do not work (7, 28). Although amino acids within the last 40 or so residues of human AGT were shown to be necessary for its peroxisomal targeting, they were still not sufficient for the peroxisomal targeting of reporter proteins (7, 12). This suggests that any additional peroxisomal targeting information in human AGT must extend beyond the C-terminal 40 amino acids. Surprisingly, this extra information is evidently absent from *Xenopus* AGT, despite being 66% identical (and 75% similar) to human AGT. This was shown by the observation that, although cytosolic *Xenopus* AGT could be redirected to the peroxisomes if its C-terminal KKM was replaced by SKL, it could not if it was replaced by KKL (28).

Although the crystal structure of the TPR domain of human Pex5p has been solved (15), the structures of very few of its cargo proteins have been determined. Therefore, it is not clear to what extent parts of the cargo, other than the C-terminal tripeptide, might interact with the import receptor and affect its function, particularly the acceptability of different C-terminal tripeptides as PTS1s. We have recently solved the crystal structure of human AGT to 2.5 Å and shown it to exist as an intimate dimer composed of two identical subunits, each of which can be divided into an N-terminal extension of about 20 amino acids, a large domain of about 260 amino acids containing most of the active site and the dimerization interface, and a smaller C-terminal domain of about 110 amino acids of uncertain function (36) (Fig. 1). The structures of AGTs from other species are likely to be very similar to that of human AGT, thereby allowing the properties of their PTS1s to be analyzed in terms of the overall protein structure, rather than just in terms of polypeptide sequence.

In the present study, we have attempted to localize the putative ancillary peroxisomal targeting information in human AGT by expression of a wide variety of AGT-GFP and interspecies AGT constructs in COS cells and determining their distribution by confocal (immuno)fluorescence microscopy. In addition, we have re-analyzed the interaction between human AGT and human Pex5p, using the mammalian two-hybrid system.

MATERIALS AND METHODS

Expression Constructs—The oligonucleotide primers used in the present study were synthesized by MWG Biotech (Germany) and are described in the Supplementary Materials. The expression constructs, cloned into either pcDNA3 (Invitrogen) or pEGFP (BD Biosciences), are described in Table I.

GFP-oligopeptide Constructs—The GFP constructs encoding C-terminal AGT penta- or hexapeptides were made using PCR with primers that annealed to the 5′ and 3′ ends of the GFP coding sequence. The 3′ primers additionally contained coding sequence for the desired C-terminal AGT oligopeptides (see Supplementary Materials). pEGFP.N3 (BD Biosciences) was used as template for PCR amplification of GFP for all GFP-oligopeptide constructs, except GFP-PKKKL for which the template was GFP-SKL (8). Reverse primers used were P23 for GFP-CPKNKL, P24 for GFP-CPRHRL, P25 for GFP-PKSKL, P26 for GFP-CAQSQL, P27 for GFP-PKKKL, and P38 for GFP-CSRNKL. Each of these reverse primers was paired with the forward primer P22, which anneals upstream of the multiple cloning site in pEGFP.N3 or in the construct GFP-SKL. The resulting PCR products were digested with XbaI at the restriction site that was introduced by the reverse primers, and BamHI at the restriction site in the multiple cloning site downstream of the P22 primer. The resulting DNA sequence fragments were ligated into BamHI-XbaI-digested pcDNA3.

GFP-AGT Constructs—GFP-*Hs*AGT-KKL was made by first producing the intermediate construct pcDNA3.GFP as follows. The region coding for SKL in GFP-SKL was replaced by an XhoI restriction site by PCR amplification using primers P34 and P35. The PCR product was then subcloned into pcDNA3 using the restriction sites KpnI at the 5′ end and XbaI at the 3′ end (outside the newly constructed XhoI site in the insert) to give pcDNA3.GFP. Human AGT was amplified from the template pAGT (*Hs*AGT-KKL in Bluescript KS+) (6) using the primers P36 and P37. The PCR product was cut with XhoI and XbaI and cloned into XhoI-XbaI-digested pcDNA3.GFP to give GFP-*Hs*AGT-KKL.

To make GFP-*Hs*$AGT_{346–392}$-KKL, the appropriate region of AGT was amplified by PCR from pAGT using primers P19 and P20. The PCR product was digested with XhoI and XbaI and cloned into the intermediate construct pcDNA3.GFP (see above). GFP-*Hs*$AGT_{361–392}$-KKL was also made from pAGT using primers P20 and P21. The PCR product was digested with BsrGI and XbaI and cloned into the intermediate construct pcDNA3.GFP. To make GFP-*Hs*$AGT_{283–392}$-KKL, the appropriate region of AGT was amplified by PCR from *Hs*AGT-KKL (8), using the primers P11 and P18. The PCR product was cut with XhoI and BspEI and cloned into XhoI-BspEI digested pEGFP.C3 (BD Biosciences).

Mammalian AGT-KKL Constructs—The rat, guinea pig, rabbit, and cat AGT-KKL and the cat AGT-CPKKKL constructs were made using the appropriate species-specific cDNAs as templates for PCR, and primers (Supplementary Materials) that introduced restriction sites for cloning and, for the reverse strand primers, changed the species-specific C-terminal tripeptides to KKL and the C-terminal hexapeptide into CPKKKL. Primers P28 and P29 were used to amplify guinea pig AGT-KKL, P30 and P31 were used for rat AGT-KKL, P6 and P7 were used for rabbit AGT-KKL, P32 and P33 were used for cat AGT-KKL, and P32

Downloaded from http://www.jbc.org/ at Murdoch University (CAUL) on May 5, 2019

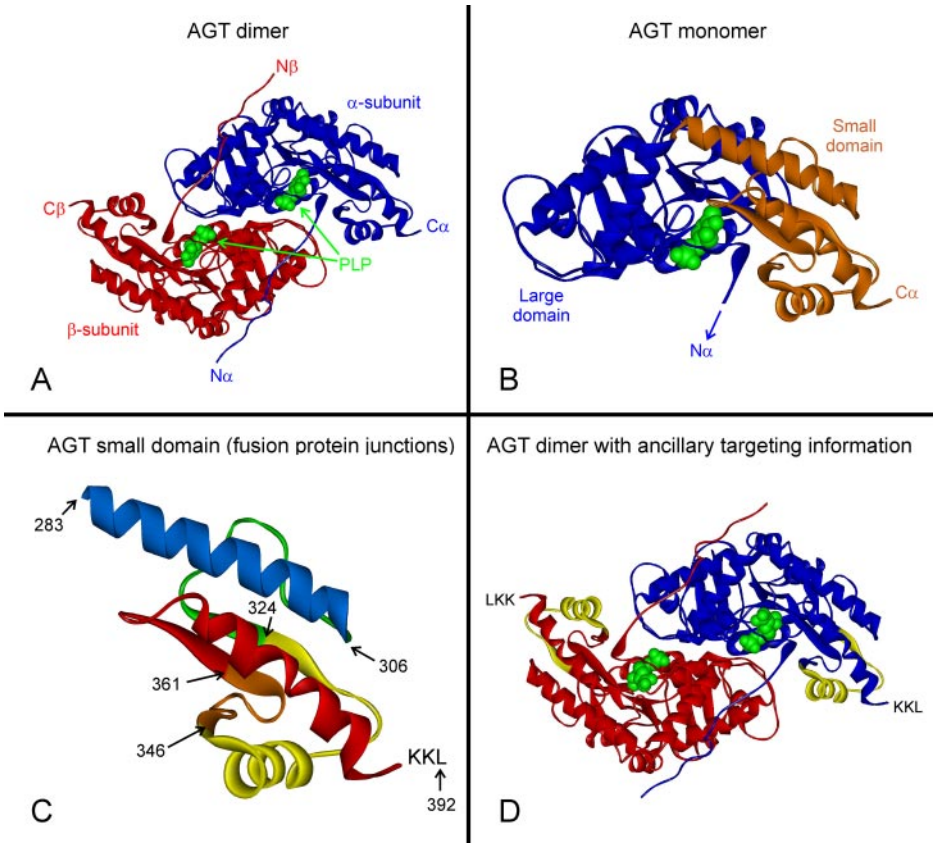

FIG. 1. **Crystal structure of human AGT.** *A–D*, the crystal structure of human AGT (36). *A*, overall topology of the AGT homodimer. The subunits are arbitrarily designated α (*blue*) and β (*red*). PLP (*green*) indicates the positions of the cofactor pyridoxal phosphate. *B*, a magnified view of the α subunit showing the large N-terminal structural domain (*blue*) and the small C-terminal structural domain (*brown*). *C*, a magnified view of the small domain indicating the various *Xenopus*-human AGT and GFP-human AGT fusion protein junctions discussed in the text, the segments being arbitrarily color-coded. The *numbers* indicate the position of the more C-terminal of the pair of residues at the junctions. The last residue identifiable in the crystal structure is 390; therefore, the C-terminal KKL indicated simply represents the approximate location of the C terminus of AGT. *D*, the whole AGT homodimer color coded as in *A* except for the putative ancillary targeting domain Val^{324}–Ile^{345} which is shown in *yellow*.

TABLE I
Description of the AGT expression constructs used in the present study

Construct	Description
*Hs*AGT-KKL[a]	Human (*H. sapiens*) AGT encoded by the more common major *AGXT* allele (8); C terminus = KKL
*Hs*AGT-SKL[b]	Human AGT in which the C-terminal KKL is replaced by SKL (7)
*Hs*AGT-KKM[b]	Human AGT in which the C-terminal KKL is replaced by KKM (28)
*Hs*AGT-ΔΔΔ[b]	Human AGT in which the C-terminal KKL is deleted (7)
*Xl*AGT-KKM	*Xenopus* (*X. laevis*) AGT encoded by the short transcript (28); C terminus = KKM
*Xl*AGT-KKL	*Xl*AGT encoded by the short transcript in which the C-terminal KKM is replaced by KKL (28)
*Xl*AGT-SKL	*Xl*AGT encoded by the short transcript in which the C-terminal KKM is replaced by SKL (28)
*Hs*283*Xl*-KKL	Residues 1–282 of *Hs*AGT fused to residues 282–389 of *Xl*AGT with a C-terminal KKL[c]
*Hs*283*Xl*-SKL	Residues 1–282 of *Hs*AGT fused to residues 282–389 of *Xl*AGT with a C-terminal SKL[c]
*Xl*283*Hs*-KKL	Residues 1–281 of *Xl*AGT fused to residues 283–392 of *Hs*AGT[c]
*Xl*306*Hs*-KKL	Residues 1–304 of *Xl*AGT fused to residues 306–392 of *Hs*AGT[c]
*Xl*324*Hs*-KKL	Residues 1–322 of *Xl*AGT fused to residues 324–392 of *Hs*AGT[c]
*Xl*361*Hs*-KKL	Residues 1–359 of *Xl*AGT fused to residues 361–392 of *Hs*AGT[c]
GFP-*Hs*AGT-KKL	GFP fused to *Hs*AGT
GFP-*Hs*$AGT_{283–392}$-KKL	GFP fused to residues 283–392 of *Hs*AGT
GFP-*Hs*$AGT_{346–392}$-KKL	GFP fused to residues 346–392 of *Hs*AGT
GFP-*Hs*$AGT_{361–392}$-KKL	GFP fused to residues 361–392 of *Hs*AGT
GFP-PKKKL	GFP fused to residues 388–392 of *Hs*AGT (*i.e.* C-terminal 5 amino acids of *Hs*AGT)
GFP-PKSKL	GFP fused to the pentapeptide PKSKL
GFP-CPRHRL	GFP fused to the C-terminal 6 amino acids of guinea pig AGT
GFP-CPKNKL	GFP fused to the C-terminal 6 amino acids of rat/mouse AGT
GFP-CSRNKL	GFP fused to the C-terminal 6 amino acids of cat AGT
GFP-CAQSQL	GFP fused to the C-terminal 6 amino acids of rabbit AGT
*Rn*AGT-KKL	Rat (*R. norvegicus*)AGT in which the normal C-terminal tripeptide (NKL) is replaced by KKL
*Cp*AGT-KKL	Guinea pig (*C. porcellus*) AGT in which the normal C-terminal tripeptide (HRL) is replaced by KKL
*Oc*AGT-KKL	Rabbit (*Oryctolagus cuniculus*) AGT in which the normal C-terminal tripeptide (SQL) is replaced by KKL
*Fc*AGT-KKL	Cat (*F. cattus*) AGT in which the normal C-terminal tripeptide (NKL) is replaced with KKL
*Fc*AGT-(CPK)KKL	Cat (*F. cattus*) AGT in which the normal C-terminal hexapeptide (CSRNKL) is replaced with CPKKKL

[a] This construct (fused to the GAL4 DNA-binding domain) was also used for the mammalian two-hybrid studies.
[b] These constructs (fused to the GAL4DNA-binding domain) were used only for the mammalian two-hybrid studies.
[c] A single human AGT subunit contains 392 amino acids, whereas *Xenopus* AGT contains 391 amino acids. As a result, residues 282 and283, which are at the junction of the large N-terminal and small C-terminal structural domains of human AGT, are equivalent to residues 281 and 282 in *Xenopus* AGT.

and P39 were used for cat AGT-CPKKKL. Guinea pig and rat AGT-KKL were subcloned into BamHI-XhoI-digested pcDNA3. Rabbit AGT-KKL, cat AGT-KKL, and cat AGT-CPKKKL were subcloned into KpnI-EcoRI-digested pcDNA3.

Xenopus-human AGT Chimeric Constructs—The chimeric *Xenopus*-human AGT constructs were produced by PCR using the method of "site-specific mutagenesis by overlap extension" (37). The two species-specific fragments were amplified separately (16 PCR cycles), using

Downloaded from http://www.jbc.org/ at Murdoch University (CAUL) on May 5, 2019

species-specific non-overlapping primers upstream or downstream of the chimeric junction, and a dual species overlapping primer at the junction. To make *Hs*283*Xl*-KKL, primers P1 and P2 were used with template *Hs*AGT-KKL and primers P3 and P4 were used with template *Xl*AGT-KKL (28). For *Xl*283*Hs*-KKL, primers P8 and P9 were used with template *Xl*AGT-KKL and primers P10 and P11 were used with template *Hs*AGT-KKL. For *Xl*306*Hs*-KKL, primers P8 and P12 were used with template *Xl*AGT-KKL and primers P13 and P11 were used with template *Hs*AGT-KKL. For *Xl*324*Hs*-KKL, primers P8 and P14 were used with template *Xl*AGT-KKL and primers P15 and P11 were used with template *Hs*AGT-KKL. For *Xl*361*Hs*-KKL, primers P8 and P16 were used with template *Xl*AGT-KKL and primers P17 and P11 were used with template *Hs*AGT-KKL. The two amplified fragments, one human and one *Xenopus*, were then mixed and subjected to a further 10 PCR cycles without primers to anneal the two fragments at the junctional overlap and extend each to the end. The products of this procedure served as templates for a final PCR round of 16 cycles, with primers P8 and P11 for the various *Xl-Hs*-KKL chimeras, and P1 with P4 for the single *Hs-Xl*-KKL chimera. The final PCR products were digested with KpnI and XhoI and cloned into pcDNA3. The construct *Hs*283*Xl*-SKL was produced by PCR amplification using primers P1 and P5 with template *Hs*283*Xl*-KKL and subcloning into KpnI-XhoI-digested pcDNA3. All constructs were checked by DNA sequencing for their correct DNA sequence (MWG Biotech).

Mammalian Two-hybrid Constructs—The positive control vector pM3-VP16, expressing a fusion of the GAL4 DNA-binding domain (BD) to the VP16 activation domain (AD) and the pG5CAT chloramphenicol acetyl transferase reporter vector were purchased from Clontech/BD Biosciences. Normal human AGT and human AGT in which the C-terminal tripeptide KKL was replaced by SKL were amplified by PCR from the template pAGT (*Hs*AGT-KKL in Bluescript KS+) (6) using the primers P40 with P41 (*Hs*AGT-KKL) and P40 with P42 (*Hs*AGT-SKL). The PCR products were cut with the restriction enzymes EcoRI and XbaI and then ligated into the vector pM GAL4 DNA-binding, which was cut with the same restriction enzymes. Human AGT in which C-terminal tripeptide KKL was replaced by KKM and human AGT in which the C-terminal three amino acids were deleted were amplified by PCR from the template *Hs*AGT-KKL using the primers P40 with P43 (*Hs*AGT-KKM) and P40 with P44 (*Hs*AGT-DDΔ). The PCR products were cut with the restriction enzymes EcoRI and SalI and then ligated into the vector pM GAL4 DNA-binding, which was cut with the same restriction enzymes. The final constructs were sequence-verified. pVP Pex5S and pVP Pex5L were produced by cutting the vectors pPTS1-BP and pGAD424-pas10, respectively (38), with BglII, filling in the recessed ends with Klenow polymerase and then cutting out the insert with SalI. These inserts were purified and ligated into pVP16 (Clontech/BD Biosciences), which was cut with HindIII, then filled in with Klenow polymerase followed by a second restriction digest with SalI.

Mammalian Two-hybrid System—To study the interaction between AGT and the PTS1 import receptor Pex5p, we used COS-1a cells and the Clontech Mammalian Matchmaker Two-Hybrid Assay Kit, as per the manufacturer's instructions. COS cells were seeded into 25-cm^2 flasks at a density of 1.2×10^4 cells per cm^2. After 24-h incubation at 37 °C, the cells were transfected as follows. Serum- and antibiotic-free Dulbecco's modified Eagle's medium (Invitrogen) was mixed with 5.5 μg of DNA, composed of 2.5 μg of each, the mammalian DNA BD, and the AD vector plus 0.5 μg of the reporter vector to a final volume of 140 μl. SuperFect (25 μl, Qiagen) was added to the DNA in the medium, and the mixture was incubated at room temperature (22–24 °C) for 5–10 min. Complete medium (1 ml containing 10% v/v fetal bovine serum and antibiotics) was then added to the mix, and the total was placed onto the cells in the flasks. The cells were incubated at 37 °C for 2–3 h; the DNA-SuperFect mixture was then removed; the cells were washed once with 5 ml of PBS, and 5 ml of the complete medium was added. The cells were then cultured for 24–48 h at 37 °C in growth medium (specification see above), after which they were harvested and extracted as follows. Cells were washed 5× with 5 ml of PBS. Fresh PBS, 250 μl, was added, and the cells were scraped off the flask surface with a rubber scraper. The cell suspension was transferred into a 0.5-ml Eppendorf tube, and the PBS was removed after centrifuging at 13,000 rpm in a microcentrifuge for 10 s. Cells were resuspended in 250 μl of 0.1 M Tris buffer, pH 7.5, containing 0.5% Triton X-100, and the mixture was incubated for 15 min on ice. The cell mixtures were then centrifuged at 13,000 rpm in a microcentrifuge at 4 °C for 5 min, and the supernatant was mixed with 4% SDS and 10% 2-mercaptoethanol in 0.125 M Tris buffer, pH 6.8, heated to 95 °C for 5 min and electrophoresed on a 8% reducing polyacrylamide gel. Separated products were visualized by immunoblotting using polyclonal rabbit anti-chloramphenicol acetyltransferase antibody (Sigma).

Cell Culture and Transfection—COS-1a cells grown to 80% confluence in growth medium (Dulbecco's modified Eagle's medium with GlutaMAX, 4500 mg/D-glucose, sodium pyruvate, 50 units/ml penicillin, 50 μg/ml streptomycin) were trypsinized and plated out onto 13-mm glass coverslips in 4-well plates at a concentration of 2.5×10^4 cells per cm^2. After 24-h incubation at 37 °C, the cells were transfected as follows. Serum- and antibiotic-free Dulbecco's modified Eagle's medium (Invitrogen) was mixed with 1–2 μg of DNA to a final volume of 60 μl. SuperFect (6 μl) (Qiagen, Crawley, West Sussex, UK) was added to the DNA in the medium and the mix was incubated at room temperature (22–24 °C) for 5–10 min. Complete medium (400 μl containing 10% v/v fetal bovine serum and antibiotics) was then added to the mix and the total was placed onto the cells on the coverslips. The cells were incubated at 37 °C for 2–3 h; the DNA-SuperFect mix was then removed; the cells were washed once with 500 μl of PBS, and 1 ml of the complete medium was added. The cells were then cultured for 24–48 h at 37 °C in growth medium (see above), after which they were processed for (immuno)fluorescence microscopy.

(Immuno)fluorescence Microscopy—The cells were fixed in freshly prepared 3% (w/v) paraformaldehyde, permeabilized in 1.0% (w/v) Triton X-100 in PBS, and immunolabeled as described previously (5–7). In some experiments, Triton X-100 was replaced by 25 μg/ml digitonin. The constructs were visualized either by the autofluorescence of GFP or by using rabbit anti-human AGT antiserum and fluorescein isothiocyanate-conjugated goat anti-rabbit IgG (Sigma). The peroxisomal marker catalase was visualized using guinea pig anti-human catalase antiserum followed by biotinylated goat anti-guinea pig IgG and Texas Red-avidin DCS (Vector, Peterborough, UK). The fluorescence of fluorescein and GFP was observed using excitation and emission wavelengths of 488 and 522 nm, respectively. For Texas Red, excitation and emission wavelengths of 568 and 605 nm, respectively, were used. The fluorescence images were captured using a confocal laser-scanning fluorescence microscope, either the MRC 1024 or the Radiance 2100 Upright Multiphoton (Bio-Rad).

The subcellular localization of the various constructs was quantified by counting cells that labeled for both the construct and peroxisomal catalase. The distribution of the construct was assessed and then categorized into either peroxisomal, peroxisomal plus cytosolic, or cytosolic. On average 302 cells (range 19–1173) were counted for each construct.

RESULTS

Human AGT Interacts with Human Pex5p in Mammalian, but Not Yeast, Cells—Previous studies have yielded conflicting results regarding the peroxisomal import pathway taken by human AGT. Although import in transfected mammalian tissue culture cells is dependent on expression of Pex5p, no interaction between AGT and human Pex5p is detectable in the yeast two-hybrid system (see the introduction). To check whether the latter result was an artifact of the heterologous system used, we have retested the interaction in the present study using a mammalian two-hybrid system. The results in Fig. 2, show clearly that *Hs*AGT-KKL does interact with *Hs*Pex5p (both long and short forms) in COS cells. Notwithstanding the qualitative, or at best semi-quantitative, nature of the two-hybrid reaction, it appeared that the strength of the interaction between *Hs*AGT-KKL and *Hs*Pex5p was similar to that of *Hs*AGT-SKL. On the other hand, two AGT constructs mutated at the C terminus, *Hs*AGT-KKM (28) and *Hs*AGT-ΔΔΔ (7), which are known not to be targeted to peroxisomes, did not interact with either form of Pex5p.

C Termini of Rat/Mouse and Guinea Pig AGTs, but Not Human, Rabbit, or Cat AGTs, Are Sufficient to Direct the Peroxisomal Import of GFP—Previous studies have shown that the human PTS1 KKL is not able to target the reporter proteins chloramphenicol acetyl-transferase and firefly luciferase to peroxisomes (7). On the other hand, a 15-mer oligopeptide ending in SQL (the C-terminal tripeptide of rabbit AGT) was able to target GFP to peroxisomes (16). To assess the peroxisomal targeting ability of the different mammalian AGT C termini, various GFP constructs were expressed in COS cells,

Downloaded from http://www.jbc.org/ at Murdoch University (CAUL) on May 5, 2019

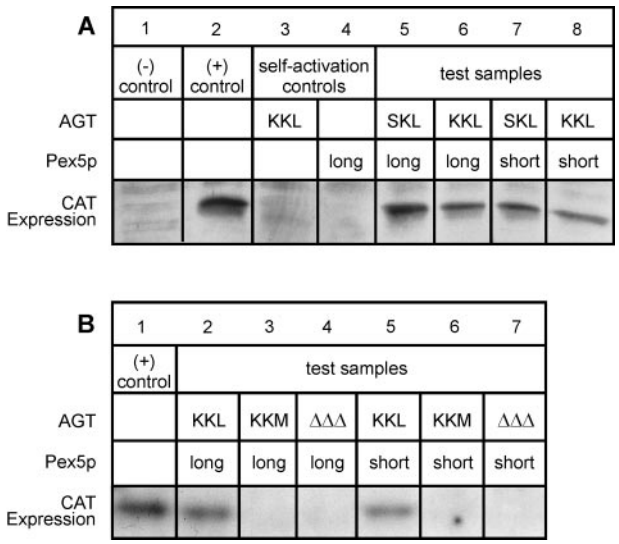

FIG. 2. **Interaction of *Hs*AGT with *Hs*Pex5p in the mammalian two-hybrid system.** The two-hybrid reaction was carried out in COS-1a cells using the Clontech Mammalian Matchmaker Two-Hybrid Assay Kit. *Hs*AGT-KKL, *Hs*AGT-SKL, *Hs*AGT-KKM, and *Hs*AGT-ΔΔΔ were fused to the DNA-binding domain, and the long and short forms of *Hs*Pex5p were fused to the activation domain. *A* and *B*, show the results from two different experiments. The results show that both *Hs*AGT-KKL and *Hs*AGT-SKL interact strongly with both long and short *Hs*Pex5p, as measured by expression of chloramphenicol acetyltransferase (*CAT*). However, neither *Hs*AGT-KKM nor *Hs*AGT-ΔΔΔ interact with either form of Pex5p. The overall expression of AGT and Pex5p was similar in all test samples (data not shown).

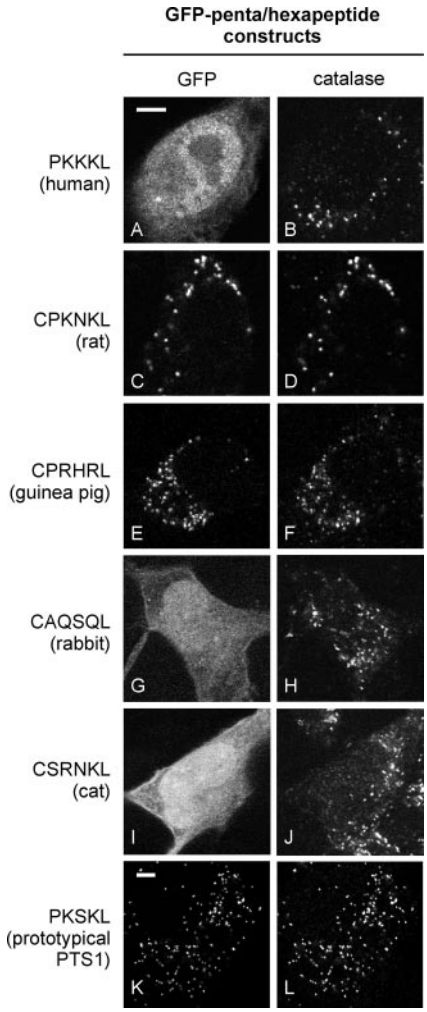

FIG. 3. **(Immuno)fluorescence analysis of the subcellular distribution of various GFP-AGT constructs in transfected COS cells.** COS cells were transfected with the following constructs: *A* and *B*, GFP-PKKKL (human); *C* and *D*, GFP-CPKNKL (rat); *E* and *F*, GFP-CPRHRL (guinea pig); *G* and *H*, GFP-CAQSQL (rabbit); *I* and *J*, GFP-CSRNKL (cat); and *K* and *L*, GFP-PKSKL (prototypical PTS1) (see Table I for a description of the constructs). After 48 h the cells were labeled and then visualized for the autofluorescence of GFP (*A*, *C*, *E*, *G*, *I* and *K*) and the peroxisomal marker catalase (*B*, *D*, *F*, *H*, *J* and *L*). *Scale bars* = 5 μm (*A–J* are the same magnification, as are *K* and *L*). GFP-PKKKL, GFP-CAQSQL, and GFP-CSRNKL were distributed diffusely in the cytosol and sometimes the nucleus; GFP-CPKNKL and GFP-CPRHRL were mainly punctuate and co-localized with catalase (*i.e.* peroxisomal). Not surprisingly, GFP-PKSKL was also strongly peroxisomal.

and the distribution was determined by fluorescence confocal microscopy. The results showed that, whereas GFP-CPKNKL (rat/mouse), GFP-CPRHRL (guinea pig), and GFP-PKSKL (prototypical PTS1) were targeted to peroxisomes, GFP-PKKKL (human/marmoset), GFP-CAQSQL (rabbit), and GFP-CSRNKL (cat) remained cytosolic (Figs. 3 and 7 (*a–f*) and Table II). During the course of these experiments, it was noticed that a substantial proportion (~85%) of cells expressing GFP-CSRNKL did not express punctuate catalase. The reason for this is unclear, but in any case GFP in these cells was entirely cytosolic frequently with significant aggregation (see Fig. 7f^2). Although GFP-CSRNKL was also mainly cytosolic (but without aggregation) in the 15% of expressing cells that did contain punctuate catalase, a minority was clearly peroxisomal (see Fig. 7f^1). Overall, these experiments showed that the C-terminal hexapeptides of rat/mouse and guinea pig AGTs were sufficient to target GFP to peroxisomes, those of human/marmoset, rabbit, and cat were not.

KKL Is Able to Target Human, Rat, Guinea Pig, and Rabbit AGTs, but Not Cat and Xenopus AGTs, to Peroxisomes—We have proposed previously that human AGT, but not *Xenopus* AGT, might contain additional peroxisomal targeting information (see above). To test whether this extra information is unique to human AGT or whether it is a common feature of mammalian AGTs, we have examined whether KKL is able to direct the peroxisomal import of other mammalian AGTs by substituting it for the naturally occurring C-terminal tripeptides in rat, guinea pig, rabbit, and cat AGTs. The results showed that KKL could direct the peroxisomal targeting of rat, guinea pig, and rabbit AGTs, as well as human AGT, but it could not do so for cat AGT (Figs. 4 and 7 (*g–k*) and Table II). The failure of KKL to target cat AGT to peroxisomes appeared to be due to an incompatibility between this tripeptide and the amino acids immediately upstream in cat AGT (*i.e.* CSR), because the C-terminal hexapeptide of human AGT (*i.e.* CPKKKL) was able to target the feline protein to peroxisomes (Figs. 4 (*I* and *J*) and 7j^2). These results suggest that ancillary peroxisomal targeting information is present in all mammalian AGTs, including that of the cat.

A Large Extended C-terminal Region of Human AGT Is Required to Direct the Peroxisomal Targeting of GFP—Numerous studies have shown that the efficiency of the Pex5p-dependent import of peroxisomal proteins can be influenced by the presence of particular residues within 10–20 amino acids of the C terminus (see the introduction). To determine the minimum contiguous sequence necessary to target human AGT to peroxisomes, we have fused full-length and variously truncated C-terminal fragments of human AGT to the C terminus of GFP and determined their subcellular distribution in transfected COS cells. The results showed that full-length human AGT, and its small C-terminal structural domain of 110 amino acids (residues 283–392) were able to target GFP to peroxisomes (Figs. 5 (*A–D*) and 7 (*l* and *m*)). However, GFP fusion constructs containing smaller amounts of AGT C-terminal sequence (*i.e.*

Downloaded from http://www.jbc.org/ at Murdoch University (CAUL) on May 5, 2019

TABLE II
C termini of AGT and peroxisomal targeting

Species	C-terminal hexapeptide	Does full-length AGT target to peroxisomes?	Can C-terminal penta/ hexapeptides direct the peroxisomal import of GFP fusions?	Does replacement of the natural C-terminal tripeptide by KKL still allow peroxisomal import of full-length AGT?
Human/marmoset	CPKKKL	Yes	No	Yes
Rat/mouse	CPKNKL	Yes	Yes	Yes
Guinea pig	CPRHRL	Yes	Yes	Yes
Rabbit	CAQSQL	Yes	No	Yes
Cat	CSRNKL	Yes[a]	No	No[b]
Dog	CPRHKL	Yes[c]	?	?
Cow	CPRSKL	?[d]	?[e]	?
Xenopus	CPKKKM	No	No	No

[a] The majority of AGT is targeted to the mitochondria in cat hepatocytes due to the presence of an N-terminal MTS. Internal translation leads to a shorter polypeptide missing the MTS, which is targeted to the peroxisomes.
[b] The human C-terminal tripeptide KKL cannot direct cat AGT to peroxisomes, because it is inhibited by residues −6 to −4 (*i.e.* CSR). However, the human C-terminal pentapeptide PKKKL can direct cat AGT to peroxisomes, because CPK at −6 to −4 is compatible with KKL.
[c] The distribution in dog is similar to that of the cat. It is likely that internal translation produces the polypeptide that is targeted to peroxisomes, as in the cat.
[d] The distribution of AGT in the cow is unknown. However, in other artiodactyls it is both mitochondrial and peroxisomal.
[e] The ability of the C terminus of cow AGT to target GFP to peroxisomes has not been formally tested. However, in numerous experiments SKL has been shown to be able to target reporter proteins to peroxisomes unless an acidic amino acid is in close proximity.

residues 346–392 and 361–392) were not (Figs. 5 (*E–H*) and 7 (*n* and *o*)).

Human-Xenopus AGT Chimeras Suggest That the Putative Additional Peroxisomal Targeting Information in Human AGT Is Located in a Region of the C-terminal Small Structural Domain of AGT Remote from Its C Terminus—A complicating factor in the GFP fusion experiments above was that several of the constructs showed a tendency to aggregate when expressed in COS cells. Because conformational stability appeared to have been compromised and might have affected targeting secondarily, we sought another system that was likely to maintain AGT structure. *Xenopus* and human AGTs are almost certainly structurally conserved, and we considered that *Xenopus*-human AGT fusion proteins would be much less prone to conformational instability and aggregation than GFP-AGT fusion proteins.

Taking advantage of the likely absence of the ancillary peroxisomal targeting information in *Xenopus* AGT, we constructed a series of human-*Xenopus* chimeric fusion proteins, containing varying amounts of human and *Xenopus* sequence, and determined their subcellular distribution in transfected COS cells. The results confirmed the GFP fusion studies above that showed that the totality of the peroxisomal targeting information of human AGT resides in the small C-terminal structural domain. This was shown by the fact that, whereas the chimera containing the large domain of *Xenopus* AGT and the small domain of human AGT (*Xl*283*Hs*-KKL) was peroxisomal, the parallel construct in which the domains were swapped over (*i.e. Hs*283*Xl*-KKL) remained mainly cytosolic (Figs. 6 (*C–F*) and 7 (*s* and *w*)). The failure of the latter construct to target to peroxisomes to any great extent was unlikely to be due to conformational obscuring of the C-terminal PTS1, because the equivalent construct in which the C-terminal KKL was replaced by SKL (*i.e. Hs*283*Xl*-SKL) was targeted efficiently to peroxisomes (Figs. 6 (*G–H*) and 7*x*).

The small structural domain consists of 110 amino acids. To narrow down the minimum sequence necessary for peroxisomal targeting, we tested the ability of a further three chimeric molecules containing decreasing amounts of human AGT small domain (*i.e. Xl*306*Hs*-KKL, *Xl*324*Hs*-KKL, and *Xl*361*Hs*-KKL) to target to peroxisomes in transfected COS cells (see Fig. 1*C* for a visualization of these constructs in the context of the crystal structure of human AGT). The results (Figs. 6 (*I–N*) and 7 (*t–v*)) showed that the efficiency with which these constructs targeted to peroxisomes decreased as the proportion of human C-terminal small domain decreased. For example, *Xl*306*Hs*-KKL was imported into peroxisomes with similar efficiency to that of *Xl*283*Hs*-KKL, whereas the import efficiency for *Xl*324*Hs*-KKL was rather less, and *Xl*361*Hs*-KKL was not imported at all. When Triton X-100 permeabilization was replaced by digitonin permeabilization neither *Xl*306*Hs*-KKL nor *Xl*324*Hs*-KKL could be detected immunologically in punctuate structures (data not shown), suggesting that these constructs, at least, were imported completely into the peroxisome interior and not just stuck to the outside of the peroxisomal membrane. Although, as predicted, the *Xenopus*-human chimeric AGTs were much more stable and less prone to aggregate than were the GFP-AGT fusions, the *Xl*361*Hs*-KKL construct did show some signs of aggregation. Other evidence in support of the conclusion that all but the last chimeric construct folded properly was provided by the fact that they all appeared to dimerize as normal (data not shown).

DISCUSSION

Cell Context Dependence of the Interaction between Human AGT and Human Pex5p—The fact that human AGT is able to interact with human Pex5p in mammalian cells (this study), but is unable to do so in yeast cells (8), suggests that, unlike for other PTS1 proteins, the correct cellular environment is important for AGT. The most likely explanation for this is that the mammalian cell provides something that the yeast cell does not. From our previous work (8), we suggested that the interaction between AGT and Pex5p might require the presence of an adaptor molecule. One explanation of the present two-hybrid results is that this adaptor is present in mammalian cells, but not yeast cells. The role of this putative adaptor could be to allosterically modify the TPR domain of Pex5p allowing it to accept the degenerate range of C-terminal tripeptides known to be able to direct human AGT to peroxisomes.

Location of the Ancillary Targeting Information in Human AGT—The results presented in this report on the intracellular targeting of *Xl*AGT-*Hs*AGT and GFP-*Hs*AGT fusion proteins show not only that all of the information required by human AGT to target it to peroxisomes is contained within the smaller C-terminal domain of 110 amino acids (residues 283–392), but also that the ancillary targeting information (PTS1A) is possibly concentrated in the 22-amino acid region from Val-324 to Ile-345 (see Fig. 1*C*). Although a number of studies have shown that residues in close proximity to the C-terminal tripeptide (*i.e.* within 10–20 amino acids) can influence the ability of this tripeptide to function as a PTS1 (see the introduction), we are not aware of any studies that have demonstrated a role for

Downloaded from http://www.jbc.org/ at Murdoch University (CAUL) on May 5, 2019

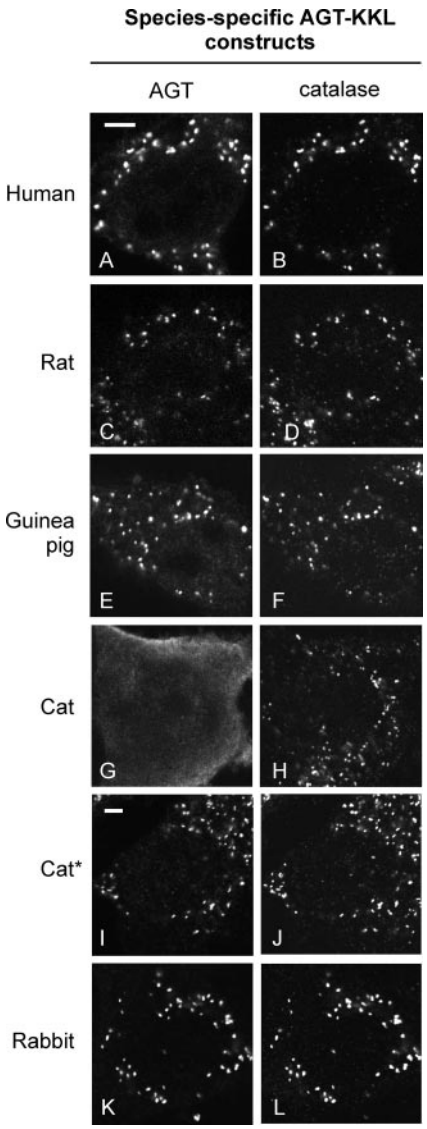

FIG. 4. **Immunofluorescence analysis of the subcellular distribution in transfected COS cells of various species-specific AGTs possessing the human C-terminal tripeptide KKL.** COS cells were transfected with the following constructs: *A* and *B*, *Hs*AGT-KKL (*i.e.* normal human AGT); *C* and *D*, *Rn*AGT-KKL; *E* and *F*, *Cp*AGT-KKL; *G* and *H*, *Fc*AGT-KKL; *I* and *J*, *Fc*AGT-(CPK)KKL; *K* and *L*, *Oc*AGT-KKL (see Table I for a description of the constructs). After 48 h the cells were labeled and then visualized for AGT (*A*, *C*, *E*, *G*, *I*, and *K*) and the peroxisomal marker catalase (*B*, *D*, *F*, *H*, *J*, and *L*). *Scale bars*, 5 μm (*A–H* are the same magnification, as are *I–L*). Whereas *Fc*AGT-KKL was distributed diffusely (*i.e.* cytosolic), all the other constructs were mainly punctuate and co-localized with catalase (*i.e.* peroxisomal).

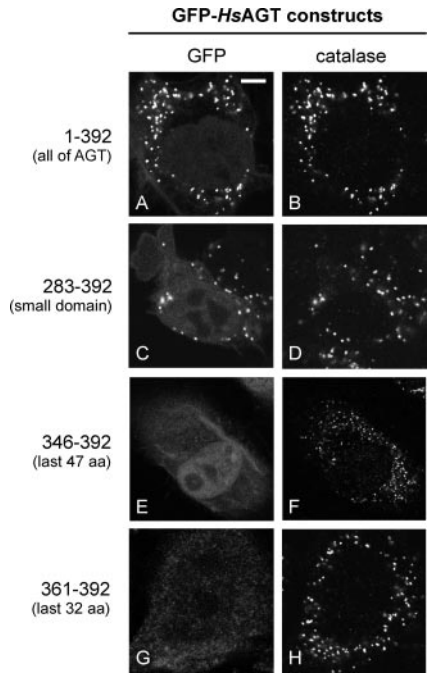

FIG. 5. **(Immuno)fluorescence analysis of the subcellular distribution of various GFP-*Hs*AGT fusions in transfected COS cells.** COS cells were transfected with the following constructs: *A* and *B*, GFP-*Hs*AGT; *C* and *D*, GFP-*Hs*AGT$_{283–392}$; *E* and *F*, GFP-*Hs*AGT$_{346–392}$; *G* and *H*, GFP-*Hs*AGT$_{361–392}$ (see Table I for a description of the constructs). After 48 h the cells were labeled and then visualized for the autofluorescence of GFP (*A*, *C*, *E*, and *G*) and the peroxisomal marker catalase (*B*, *D*, *F*, and *H*). *Scale bar* = 5 μm (all panels are at the same magnification). GFP-*Hs*AGT and GFP-*Hs*AGT$_{283–392}$ had a punctuate distribution that co-localized with catalase (*i.e.* peroxisomal). However, *Hs*GFP-AGT$_{348–392}$ and GFP-*Hs*AGT$_{361–392}$ were diffusely distributed in the cytosol and nucleus with no sign of peroxisomal labeling. All constructs, except GFP-*Hs*AGT, also show signs of aggregation in the cytosol.

residues so distant from the C terminus as found for the PTS1A in human AGT. Unfortunately, the edges of the region containing the PTS1A cannot be determined exactly. In particular, it is uncertain to what extent it extends downstream toward the C terminus. Although there is some evidence that deletions to regions between the C-terminal tripeptide and the region identified in the present study can interfere with the peroxisomal targeting of human AGT (7), it is unlikely that these intervening regions are directly involved in providing targeting information. It is more likely that these studies demonstrate the consequences of perturbation of the spatial relationship between the ancillary targeting region and the C-terminal tripeptide (see below). Even if the PTS1A is not required, major structural alterations to the intervening regions could affect PTS1 functioning. For example, some point mutations predicted to disrupt the C-terminal α-helix (residues 371–387) inhibit the peroxisomal targeting of rat AGT (33), even though we have shown in the present study that its C-terminal hexapeptide CPKNKL does not require any additional targeting information to work as a PTS1. In addition, certain point mutations upstream of the C-terminal tripeptide, especially the close proximity of acidic residues, can interfere with the peroxisomal targeting of human AGT (12), even if the C-terminal KKL is replaced by SKL, probably due to inhibiting the operation of the C-terminal PTS1 rather than due to the loss of any extra targeting information.

Cat AGT is unusual among the mammalian AGTs, because it is the only one in which the residues immediately upstream of the C-terminal tripeptide (*i.e.* CSR) appear to compromise the ability of KKL to act as a PTS1. In vertebrate AGTs, residues -4 to -6 are much better conserved than the terminal residues -1 to -3. For example, they are CPK in human/marmoset, rat/mouse, and *Xenopus* and CPR in guinea pig, dog, and cow (see Table II). The least well conserved are the rabbit (CAQ) and the cat (CSR). Although the structural basis of the cat AGT-specific interference of KKL function remains unknown, it is clearly related to the presence of serine at -5. It appears that, although closely positioned residues can prevent KKL from working as a PTS1, they cannot allow KKL to work if the PTS1A is not present. This is clearly shown by *Xenopus* AGT, the C terminus of which is almost identical to that of human AGT (CPKKKM *versus* CPKKKL, see Table II). Despite this, it cannot be directed to peroxisomes by replacing the final methionine by leucine.

The ability of KKL (or CPKKKL in the case of the cat), to

Downloaded from http://www.jbc.org/ at Murdoch University (CAUL) on May 5, 2019

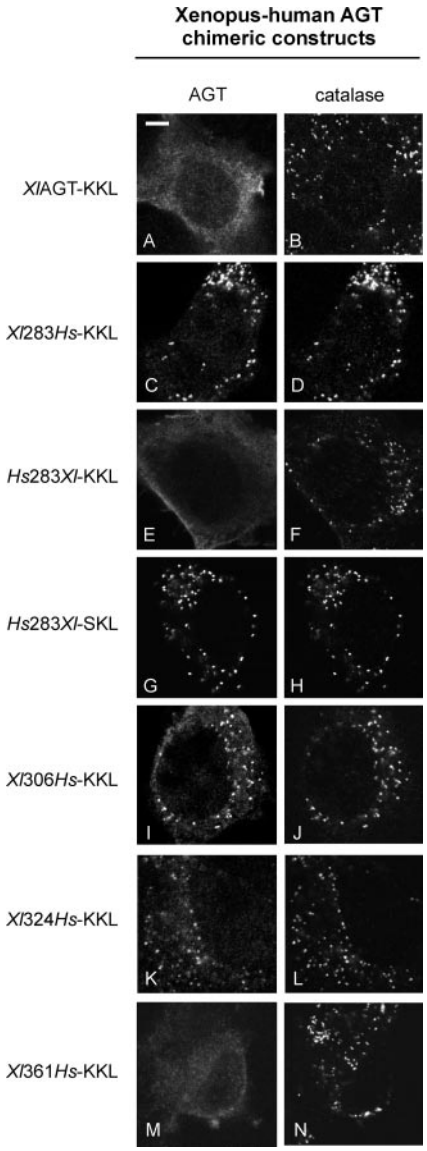

FIG. 6. **Immunofluorescence microscopic analysis of the subcellular distribution of human and *Xenopus* chimeric AGTs in transfected COS cells.** COS cells were transfected with the following constructs: *A* and *B*, *Xl*AGT-KKL; *C* and *D*, *Xl*283*Hs*-KKL; *E* and *F*, *Hs*283*Xl*-KKL; *G* and *H*, *Hs*283*Xl*-SKL; *I* and *J*, *Xl*306*Hs*-KKL; *K* and *L*, *Xl*324*Hs*-KKL; *M* and *N*, *Xl*361*Hs*-KKL (see Table I for a description of the constructs). After 48 h the cells were double-labeled for AGT (*A*, *C*, *E*, *G*, *I*, *K*, and *M*) and the peroxisomal marker catalase (*B*, *D*, *F*, *H*, *J*, *L*, and *N*). *Scale bar* = 5 μm (all panels are at the same magnification). The constructs *Xl*283*Hs*-KKL and *Hs*283*Xl*-SKL were punctuate co-localizing with catalase (peroxisomal). *Xl*306*Hs*-KKL and *Xl*324*Hs*-KKL were both diffuse (cytosolic) and punctuate co-localizing with catalase (peroxisomal). *Xl*AGT-KKL, *Hs*283*Xl*-KKL, and *Xl*361*Hs*-KKL were diffusely distributed (*i.e.* cytosolic) with no sign of punctate (peroxisomal) labeling.

target all the mammalian AGTs to peroxisomes suggests that all these mammalian AGTs possess the PTS1A, even though the GFP fusion protein results indicate that it is not required in the rodents (*i.e.* rat, mouse, and guinea pig). In *Xenopus* AGT, which does not contain a PTS1A, the region between residues 324 and 345 is much more poorly conserved compared with the same region in human AGT than is the whole protein (36% identical compared with 66%). However, this region in rat, guinea pig, rabbit, and cat AGTs is as well conserved, compared with human AGT, as is the rest of the protein (77–91% identical compared with 78–83%). This level of conservation, or lack of conservation, of this region is compatible with its ability to function as a PTS1A in mammalian AGT, but not *Xenopus* AGT.

Possible Mechanism of Action of the Ancillary Peroxisomal Targeting Information (PTS1A)—The region between Val-324 and Ile-345, which our present results suggest is the most likely candidate for the PTS1A, is exposed on the surface of the AGT dimer. Although it is 47–68 residues upstream of the C terminus, in the three-dimensional crystal structure of AGT the PTS1A and the PTS1 are very close (see Fig. 1*D*). For example, the main chain of Gly-329 is only 4.5 Å from that of Lys-389. If close proximity between residues 324–345 (the PTS1A) and residues 390–392 (the PTS1) is important, then it is not surprising that deletions or point mutations in the intervening regions that disrupt their spatial relationship should also interfere with peroxisomal targeting.

In the absence of explicit data on the crystal structure of the AGT-Pex5p import complex, the exact mechanism of action of the PTS1A remains speculative. The crystal structure of the TPR domain of human Pex5p complexed with a hexapeptide ending in SKL explains the requirement of this tripeptide, or conservative variants thereof, in the peroxisomal targeting of most peroxisomal proteins (15). However, it fails to explain how mammalian AGTs, uniquely, can be targeted to peroxisomes by KKL, SQL, NKL, HRL, SKL, SSL, and probably many other tripeptides. One possible role for the ancillary targeting information is to bind directly or indirectly to human Pex5p causing an allosteric change to the conformation of the TPR region to allow it to accept such a degenerate range of PTS1s. Our previous (8) and present studies indicate that the peroxisomal import of human AGT might require an additional factor that is present in mammalian, but not yeast, cells. Therefore, it is possible that the PTS1A in human AGT interacts with this putative additional factor, rather than human Pex5p directly. The human AGT-adaptor complex would in turn interact with human Pex5p altering the specificity of its TPR domain.

Evolutionary Origins of the PTS1A in Mammalian AGT—If our interpretation of the data presented in this and previous papers is correct, then the question remains as to why human AGT has evolved such a mechanism for peroxisomal import, whereas most other peroxisomal proteins seem able to rely on the necessity and sufficiency of the prototypical PTS1 C-terminal tripeptide. The answer probably lies in the unique evolutionary history of AGT targeting (see the introduction) (30). During vertebrate evolution, the intracellular targeting of AGT has changed on numerous occasions under the influence of dietary selection pressure. Depending on the particular species, AGT can be peroxisomal, peroxisomal and cytosolic, peroxisomal and mitochondrial, mitochondrial, or mitochondrial and cytosolic (25, 30, 39). In general, AGT is more likely to be mitochondrial the more carnivorous the diet, and more peroxisomal the more herbivorous the diet. It appears that the ultimate intracellular destination of AGT depends mainly on whether an N-terminal MTS is either included within, or excluded from, the open reading frame. The apparent hierarchical dominance of the MTS over the PTS1 would lead to low evolutionary conservation pressure on the PTS1 when the MTS is present and may thus have led to the diversity of PTS1 tripeptides observed in mammals. Early mammalian lineages were probably mainly carnivorous or omnivorous with AGT being entirely or mainly mitochondrial (30). Efficient peroxisomal targeting could have evolved on many different occasions as an adaptive response to episodic pressure for more herbivorous diets.

The prsence of the PTS1A in rodents, even though it would appear to be unnecessary, suggests that it evolved for some other reason unrelated to peroxisomal targeting. Although the crystal structure of AGT would suggest that this other function

Downloaded from http://www.jbc.org/ at Murdoch University (CAUL) on May 5, 2019

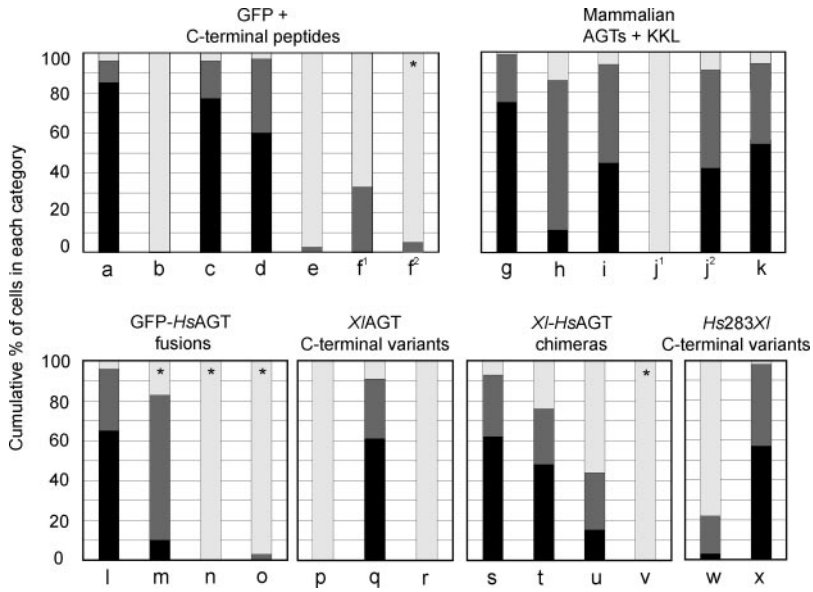

FIG. 7. **Semi-quantification of the subcellular distribution of all the AGT constructs in transfected COS cells.** The subcellular distribution was determined for each construct in an average of ~300 cells. Distribution in each cell, which expressed construct and punctate catalase, was categorized as either peroxisomal (*black*), peroxisomal and cytosolic (*dark gray*), or cytosolic (*light gray*). An *asterisk* indicates the additional presence of aggregated protein in the cytosol. The *ordinate* indicates the cumulative percentage of cells in each category. The panels are labeled as follows: *GFP + C-terminal penta/hexapeptides*: *a*, GFP-PKSKL; *b*, GFP-PKKKL (human); *c*, GFP-CPKNKL (rat); *d*, GFP-CPRHRL (guinea pig); *e*, GFP-CAQSQL (rabbit); f^1, GFP-CSRNKL (cat); f^2, same as f^1 but counting all cells, including those not containing punctuate catalase (see text). *Mammalian AGTs + KKL*: *g*, *Hs*AGT; *h*, *Rn*AGT-KKL; *i*, *Cp*AGT-KKL; j^1, *Fc*AGT-KKL; j^2, *Fc*AGT-(CPK)KKL; *k*, *Oc*AGT-KKL. *GFP-Hs*AGT fusions: *l*, GFP-*Hs*AGT; *m*, GFP-*Hs*AGT283–392; *n*, GFP-*Hs*AGT346–392; *o*, GFP-*Hs*AGT361–392. *XlAGT C-terminal variants*: *p*, *Xl*AGT-KKM; *q*, *Xl*AGT-SKL; *r*, *Xl*AGT-KKL; *Xl/HsAGT chimeras*: *s*, *Xl*283*Hs*; *t*, *Xl*306*Hs*; *u*, *Xl*324*Hs*; *v*, *Xl*361*Hs*. *Hs283Xl C-terminal variants*: *w*, *Hs*283*Xl*-KKL; *x*, *Hs*283*Xl*-SKL.

is unlikely to be related to catalytic activity, it could be involved with the stability of the enzyme. Its ability to enable otherwise inadequate PTS1s, such as KKL in human AGT, SQL in rabbit AGT, and NKL in cat AGT, to function as PTS1s might have been a chance side-effect. If the PTS1s of mammalian AGT evolved on numerous occasions, then because they evolved in the presence of the PTS1A, they did not need to evolve sufficiency. The sufficiency of rodent AGT PTS1s (*i.e.* those of rat/mouse and guinea pig) might simply result from a purely chance event occurring in their early evolutionary history. Alternatively, the ancestral rodent might have transiently lost its PTS1A, and only re-acquired it after the rodent PTS1 had evolved.

PTS1A and Kidney Stone Disease—The efficiency with which AGT is targeted to peroxisomes could be a significant determinant of an individual's susceptibility to idiopathic calcium oxalate kidney stone disease. This is suggested by the fact that a third of patients with primary hyperoxaluria type 1 have disease, because AGT is redirected away from the peroxisomes toward the mitochondria (1). In addition, some patients with peroxisome biogenesis disorders, such as Zellweger syndrome, in which AGT becomes stuck in the cytosol, have marked hyperoxaluria (40, 41). If the PTS1A, in addition to the PTS1, is a determinant of AGT peroxisomal import efficiency, then naturally occurring amino acid replacements in this region might be expected to affect this efficiency. The knock-on effect of this would be altered levels of oxalate synthesis, which could easily influence the likelihood of calcium oxalate deposition in the kidney. In this context, it is interesting to note that of the three non-synonymous polymorphisms found in human AGT (*i.e.* $Pro^{11} \rightarrow Leu$, $Val^{326} \rightarrow Ile$, and $Ile^{340} \rightarrow Met$) (42), two are located in the 22-residue PTS1A. $Ile^{340} \rightarrow Met$ segregates with the minor *AGXT* allele, which also contains $Pro^{11} \rightarrow Leu$. $Val^{326} \rightarrow Ile$ segregates with a variant called the minor (African) AGXT allele (43). Although the functional effects of the two PTS1A polymorphisms have not been well characterized, it is known that $Ile^{340} \rightarrow Met$ can partially counteract the untoward effects of the $Pro^{11} \rightarrow Leu$ polymorphism, which include partial mistargeting, slowing down dimerization, and decreasing specific catalytic activity (3, 44). In some of the mammals discussed in this report (*i.e.* guinea pig, cat, dog, and cow) residue 340 is normally methionine rather than isoleucine. Whether this has any specific effect on AGT peroxisomal targeting efficiency and oxalate synthesis in these species has yet to be determined.

REFERENCES

1. Danpure, C. J. (2001) in *The Metabolic and Molecular Bases of Inherited Disease* (Scriver, C. R., Beaudet, A. L., Sly, W. S., Valle, D., Childs, B., Kinzler, K. W., and Vogelstein, B., eds) pp. 3323–3367, McGraw-Hill, New York
2. Danpure, C. J., Cooper, P. J., Wise, P. J., and Jennings, P. R. (1989) *J. Cell Biol.* **108,** 1345–1352
3. Purdue, P. E., Takada, Y., and Danpure, C. J. (1990) *J. Cell Biol.* **111,** 2341–2351
4. Purdue, P. E., Allsop, J., Isaya, G., Rosenberg, L. E., and Danpure, C. J. (1991) *Proc. Natl. Acad. Sci. U. S. A.* **88,** 10900–10904
5. Leiper, J. M., Oatey, P. B., and Danpure, C. J. (1996) *J. Cell Biol.* **135,** 939–951
6. Lumb, M. J., Drake, A. F., and Danpure, C. J. (1999) *J. Biol. Chem.* **274,** 20587–20596
7. Motley, A., Lumb, M. J., Oatey, P. B., Jennings, P. R., De Zoysa, P. A., Wanders, R. J., Tabak, H. F., and Danpure, C. J. (1995) *J. Cell Biol.* **131,** 95–109
8. Knott, T. G., Birdsey, G. M., Sinclair, K. E., Gallagher, I. M., Purdue, P. E., and Danpure, C. J. (2000) *Biochem. J.* **352,** 409–418
9. Takada, Y., Kaneko, N., Esumi, H., Purdue, P. E., and Danpure, C. J. (1990) *Biochem. J.* **268,** 517–520
10. Gould, S. J., Keller, G. A., Hosken, N., Wilkinson, J., and Subramani, S. (1989) *J. Cell Biol.* **108,** 1657–1664
11. Swinkels, B. W., Gould, S. J., and Subramani, S. (1992) *FEBS Lett.* **305,** 133–136
12. Oatey, P. B., Lumb, M. J., Jennings, P. R., and Danpure, C. J. (1996) *Ann. N. Y. Acad. Sci.* **804,** 652–653
13. Van Der Leij, I., Franse, M. M., Elgersma, Y., Distel, B., and Tabak, H. F. (1993) *Proc. Natl. Acad. Sci. U. S. A.* **90,** 11782–11786
14. Brocard, C., Kragler, F., Simon, M. M., Schuster, T., and Hartig, A. (1994) *Biochem. Biophys. Res. Commun.* **204,** 1016–1022
15. Gatto, G. J., Geisbrecht, B. V., Gould, S. J., and Berg, J. M. (2000) *Nat. Struct. Biol.* **7,** 1091–1095
16. Lametschwandtner, G., Brocard, C., Fransen, M., Van Veldhoven, P., Berger, J., and Hartig, A. (1998) *J. Biol. Chem.* **273,** 33635–33643
17. Neuberger, G., Maurer-Stroh, S., Eisenhaber, B., Hartig, A., and Eisenhaber,

Downloaded from http://www.jbc.org/ at Murdoch University (CAUL) on May 5, 2019

F. (2003) *J. Mol. Biol.* **328,** 567–579
18. Neuberger, G., Maurer-Stroh, S., Eisenhaber, B., Hartig, A., and Eisenhaber, F. (2003) *J. Mol. Biol.* **328,** 581–592
19. Gatto, G. J., Jr., Maynard, E. L., Guerrerio, A. L., Geisbrecht, B. V., Gould, S. J., and Berg, J. M. (2003) *Biochemistry* **42,** 1660–1666
20. Purdue, P. E., Lumb, M. J., and Danpure, C. J. (1992) *Eur. J. Biochem.* **207,** 757–766
21. Birdsey, G. M., and Danpure, C. J. (1998) *Biochem. J.* **331,** 49–60
22. Oda, T., Miyajima, H., Suzuki, Y., and Ichiyama, A. (1987) *Eur. J. Biochem.* **168,** 537–542
23. Li, X. M., Salido, E. C., and Shapiro, L. J. (1999) *Somat. Cell Mol. Genet.* **25,** 67–77
24. Lumb, M. J., Purdue, P. E., and Danpure, C. J. (1994) *Eur. J. Biochem.* **221,** 53–62
25. Birdsey, G. M., Lewin, J., Cunningham, A., Bruford, M. W., and Danpure, C. J. (2004) *Mol. Biol. Evol.* **21,** 632–646
26. Danpure, C. J., Fryer, P., Jennings, P. R., Allsop, J., Griffiths, S., and Cunningham, A. (1994) *Eur. J. Cell Biol.* **64,** 295–313
27. Danpure, C. J., Guttridge, K. M., Fryer, P., Jennings, P. R., Allsop, J., and Purdue, P. E. (1990) *J. Cell Sci.* **97,** 669–678
28. Holbrook, J. D., and Danpure, C. J. (2002) *J. Biol. Chem.* **277,** 2336–2344
29. Holbrook, J. D., Birdsey, G. M., Yang, Z., Bruford, M. W., and Danpure, C. J. (2000) *Mol. Biol. Evol.* **17,** 387–400
30. Birdsey, G. M., Lewin, J., Holbrook, J. D., Simpson, V. R., Cunningham, A. A., and Danpure, C. J. (2005) *Proc. R. Soc. Lond. B.*, **272,** 833–840
31. Elgersma, Y., Vos, A., Van Den Berg, M., van Roermund, C. W., van der Sluijs, P., Distel, B., and Tabak, H. F. (1996) *J. Biol. Chem.* **271,** 26375–26382
32. Maynard, E. L., Gatto, G. J., Jr., and Berg, J. M. (2004) *Proteins* **55,** 856–861
33. Mizuno, T., Ito, K., Uchida, C., Kitagawa, M., Ichiyama, A., Miura, S., Fujita, K., and Oda, T. (2002) *Histochem. Cell Biol.* **118,** 321–328
34. Purdue, P. E., and Lazarow, P. B. (1996) *J. Cell Biol.* **134,** 849–862
35. Miura, S., Kasuya Arai, I., Mori, H., Miyazawa, S., Osumi, T., Hashimoto, T., and Fujiki, Y. (1992) *J. Biol. Chem.* **267,** 14405–14411
36. Zhang, X., Roe, S. M., Hou, Y., Bartlam, M., Rao, Z., Pearl, L. H., and Danpure, C. J. (2003) *J. Mol. Biol.* **331,** 643–652
37. Sambrook, J., and Russell, D. W. (2001) *Molecular Cloning: A Laboratory Manual*, Third Ed., Cold Spring Harbor Laboratory Press, Cold Spring Harbor, NY
38. Braverman, N., Dodt, G., Gould, S. J., and Valle, D. (1998) *Hum. Mol. Genet.* **7,** 1195–1205
39. Caldwell, E. F., Mayor, L. R., Thomas, M. G., and Danpure, C. J. (2004) *Hum. Genet.* **115,** 504–509
40. Wanders, R. J., van Roermund, C. W., Westra, R., Schutgens, R. B., van der Ende, M. A., Tager, J. M., Monnens, L. A., Baadenhuysen, H., Govaerts, L., Przyrembel, H., Wolff, E. D., Blom, W., Huijmans, J. G., and van Laerhoven, F. G. (1987) *Clin. Chim. Acta* **165,** 311–319
41. Danpure, C. J., Fryer, P., Griffiths, S., Guttridge, K. M., Jennings, P. R., Allsop, J., Moser, A. B., Naidu, S., Moser, H. W., MacCollin, M., and DeVivo, D. C. (1994) *J. Inher. Metab. Dis.* **17,** 27–40
42. Coulter-Mackie, M. B., and Rumsby, G. (2004) *Mol. Genet. Metab* **83,** 38–46
43. Coulter-Mackie, M. B., Tung, A., Henderson, H. E., Toone, J. R., and Applegarth, D. A. (2003) *Mol. Genet. Metab* **78,** 44–50
44. Lumb, M. J., and Danpure, C. J. (2000) *J. Biol. Chem.* **275,** 36415–36422

Downloaded from http://www.jbc.org/ at Murdoch University (CAUL) on May 5, 2019

Peroxisomal Import of Human Alanine:glyoxylate Aminotransferase Requires Ancillary Targeting Information Remote from Its C Terminus

Pia A. J. Huber, Graeme M. Birdsey, Michael J. Lumb, David T. R. Prowse, Tommy J. Perkins, Daniel R. Knight and Christopher J. Danpure

J. Biol. Chem. 2005, 280:27111-27120.
doi: 10.1074/jbc.M502719200 originally published online May 23, 2005

Access the most updated version of this article at doi: 10.1074/jbc.M502719200

Alerts:
- When this article is cited
- When a correction for this article is posted

Click here to choose from all of JBC's e-mail alerts

Supplemental material:
http://www.jbc.org/content/suppl/2005/05/24/M502719200.DC1

This article cites 40 references, 16 of which can be accessed free at
http://www.jbc.org/content/280/29/27111.full.html#ref-list-1

Downloaded from http://www.jbc.org/ at Murdoch University (CAUL) on May 5, 2019